GEOPHYSICAL RESEARCH LETTERS, VOL. 22, NO. 4, PAGES 353-356, FEBRUARY 15, 1995

Hybrid simulations of the saturated Farley-Buneman instability in the ionosphere

Meers Oppenheim, Niels Otani and Corrado Ronchi[1]

Space Plasma Physics Division, School of Electrical Engineering, Cornell University

Abstract. Numerical simulations of the Farley-Buneman instability in 2-1/2 dimensions using particle ions and fluid electrons show the growth, saturation and nonlinear behavior of two-stream waves. This hybrid technique models the saturated state of the instability for a much longer period of time than the pure particle codes that preceded it. While focusing principally on modeling the topside E region equatorial electrojet, many of these results apply to the auroral two-stream instability as well. The following features are seen in all our hybrid simulations: (1) wave growth at an angle offset from the electron drift direction where the angle depends on the strength of the driving electric field, (2) nonlinear coupling to waves traveling perpendicular to the propagation direction of the principal two-stream waves, (3) a saturated wave phase velocity at or above the sound speed but well below the velocity predicted by linear theory and (4) phase velocities which remain almost constant as a simulated radar sweeps from a horizontal direction to nearly vertical. The nonlinear electron motion dominates the behavior of these waves. Further, these simulations indicate that ion kinetic effects are not essential for the saturation of the instability and that electron temperature effects have a minor impact on the final saturated state.

Introduction

The equatorial electrojet is a stream of current that travels above the equator at an altitude of 90 - 120 km (called the E region). Periodically, strong radar echoes reflect from the electrojet indicating the presence of waves. *Farley* [1963] and *Buneman* [1963] used linear theory to explain some of the characteristics of these meter scale irregularities and of similar ones observed in the polar E region. Later, *Sudan et al.* [1973] and *Fejer et al.* [1984] elaborated on this theory. For a summary, see *Kelley* [1989].

The electrojet occurs at an altitude where ion-neutral collisions dominate ion behavior while both electron-neutral collisions and the Earth's magnetic field affect electron behavior. When vertical electric fields develop in response to daily tidal oscillations of the neutral atmosphere, electrons $\mathbf{E}\times\mathbf{B}$ drift horizontally while ions remain in place due to collisions with neutrals. The resulting current is called the electrojet. The Farley-Buneman (FB) instability occurs when the electron drift velocity exceeds the acoustic speed.

A number of features seen in the observational database cannot be explained by the linear FB theory. The phase velocity of the waves appears closer to the acoustic speed than the drift velocity and the waves appear to have the same phase velocity regardless of the elevation angle. Linear theory cannot predict the saturation level or explain the generation of vertical density irregularities observed by the Jicamarca radar facility in Peru. However, we observed all of these effects with our two-dimensional hybrid computer code.

This letter briefly presents the methods and results of a set of simulations of the Farley-Buneman (FB) instability for the case of pure two-stream waves with no zero order density gradient. We show that the nonlinear $\mathbf{E}\times\mathbf{B}$ electron motion dominates the behavior of the saturated waves and that electron temperature effects play only a modest role, while the magnitude of the electron drift velocity affects the system in a pronounced fashion. Furthermore, the phase velocity of the saturated waves is largely independent of the drift speed.

Simulation Methods

The linear theory of the FB instability predicts that ion Landau damping plays a crucial role in eliminating short wavelength waves, a feature neglected by a fluid model of ion behavior [*Schmidt and Gary*, 1973]. A particle-in-cell (PIC) method of modeling ion behavior allows us to include all kinetic ion effects at the expense of slow computation and substantial particle noise. Even with nearly a million particles on a 64 by 64 mesh, random fluctuations in the particle locations lead to a variation in the number of particles per cell of 2% to 3%. This level is comparable to the fully developed pure two stream waves where the driving electric field is near the minimum threshold for the instability.

Our code applies standard PIC methods to the ions with the addition of the following features. We calculate ion velocities in $3D$ while tracking ion positions and the resulting electric fields only in the plane perpendicular to the Earth's magnetic field. We model ion-neutral collisions by elastically colliding a fraction of the ions with a thermal distribution of neutral particles and use a short wavelength filter to halve the particle noise.

Our fluid model of electron behavior neglects electron inertial effects, making the shortest timescale in the simulation the electron-neutral collision rate. From the inertialess electron momentum equation, assuming an electrostatic system and quasineutrality ($\nabla\cdot\mathbf{J}=0$), one can derive the following equation in the plane perpendicular to the magnetic field ($\mathbf{B}=B_0\hat{\mathbf{y}}$):

[1]Now at: ENEA, C.R.E. Casaccia, Rome, ITALY

Paper number 94GL03277
0094-8534/95/94GL-03277$03.00

$$n\nabla^2\phi + \nabla\phi\cdot\nabla n + \kappa\hat{\mathbf{y}}\cdot\nabla\phi\times\nabla n =$$
$$\mathbf{E}_0\cdot\nabla n + \kappa\hat{\mathbf{y}}\cdot\mathbf{E}_0\times\nabla n + (T_e/e)\nabla^2 n + \Gamma\nabla\cdot\mathbf{J_i}$$
$$\kappa \equiv \Omega_e/\nu_e(\gg 1), \quad \Gamma = (m_e/e^2)(\nu_e^2+\Omega_e^2)/\nu_e \quad (1)$$

where all units are in MKS and ϕ is the potential, n is the density, Ω_e is the electron cyclotron frequency, ν_e is the electron-neutral collision rate, E_0 is the driving electric field, T_e is the electron temperature in Joules, m_e is the electron mass and J_i is the ion current determined from the ion particles.

The nonlinear term, $\kappa\hat{\mathbf{y}}\cdot\nabla\phi\times\nabla n$, in (1) is multiplied by a factor of κ which, in the case of the E region, is a large number (≈ 100). This makes the nonlinear term the same order of magnitude as the linear terms even for fairly small density variations. This nonlinear term couples only cross-propagating waves making its behavior fundamentally 2D.

Numerically solving (1) for ϕ proved very difficult. Using finite difference equations, we convert the PDE into a matrix problem, $\mathbf{Ax} = \mathbf{b}$ where $\mathbf{A}$ and $\mathbf{b}$ are known quantities. When periodic boundary conditions are applied in both directions, ϕ in (1) is determined up to an arbitrary constant. This freedom translates into a singularity in the matrix. This singularity may not be eliminated by simply fixing the potential at a single point (node) as done by *Newman and Ott* [1981], though a subtle modification of this approach does work. *Janhunen* [1992] approached this problem using a successive-over-relaxation technique which fails to converge when the nonlinear components of (1) become large, making the matrix highly non-diagonally dominant. We solved these problems by carefully reformulating the finite difference equations to eliminate the singularity and by using a variant on the biconjugate gradient method, called the quasi-minimal residual method [*Freund and Nachtigal*, 1994].

Simulation Results

Our baseline simulation attempts to represent typical conditions of the daytime equatorial electrojet at an altitude of approximately $105km$. Table 1 shows the parameters used for this simulation. In addition, we have 921600 particles, periodic boundary conditions, a total simulation size of $8m$ by $8m$ with a grid resolution of 64 by 64 and a time step of $10\mu s$. Figure 1 shows the time history of the observed density saturation level, for different values of the electron temperature and horizontal electric field. Figure 2 shows a typical saturated state of the FB waves generated by this simulation. The baseline simulation uses an artificially high driving electric field, E_{0y}, of $20mV/m$ in order to minimize the effects of particle noise. Lowering the grid resolution to 32 by 32 halves the effective particle noise enabling us to resolve waves generated by a $15mV/m$ driving electric field. With this more realistic driving field, we obtain, qualitatively, similar results to the baseline simulation.

Table 1. Baseline Simulation Parameters

Parameter (Symbol)	Value	Units
Static magnetic field ($\mathbf{B}_0$)	25	nT
Mean vertical $\mathbf{E}$ field ($\mathbf{E}_{0z}$)	-0.02	V/m
Mean Ion density (n_0)	10^{11}	m^{-3}
Neutral density (n_n)	6×10^{18}	m^{-3}
Initial Temperatures (T_*)	208	K
Effective ion mass (m_i)	4.6×10^{-26}	kg
e^--neutral collision freq. (ν_e)	4.0×10^4	s^{-1}
Ion-neutral collision freq. (ν_i)	2.8×10^3	s^{-1}

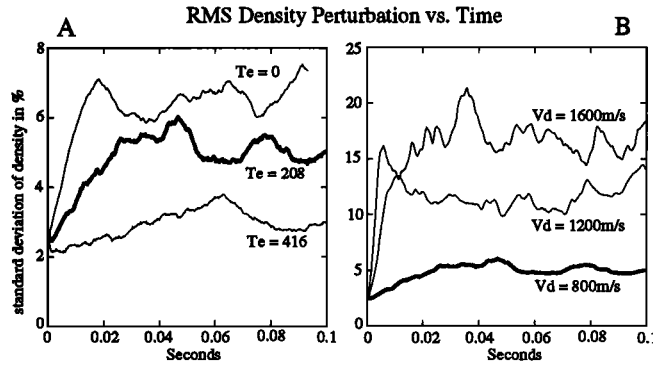

Figure 1. Time history of the standard deviation of $\delta n/n_0$ for (A) three electron temperatures with constant $V_d = 800m/s$ and $T_i = T_n = 208K$ and (B) three drift velocities with $T_e = T_i = T_n = 208K$. The baseline case is the bold line. While the growth rates shown in both (A) and (B) are below that predicted by linear theory, the relative growth rates between simulations behaves as predicted by this theory. Hence, in figure (B), the growth rate scales proportionally to the square of the drift velocity and, in (A), the growth rate scales with the negative of the square of the acoustic speed.

The dispersion plot (Figure 3) of these saturated waves yields their phase velocities and spectral widths. We estimate the phase velocity at $430m/s$. The $1D$ linear dispersion relation of the FB instability for small growth rates is

$$\omega_r = \frac{kV_d}{1+\Psi_0} \qquad \gamma = \frac{\Psi_0/\nu_i}{1+\Psi_0}(\omega_r^2 - k^2C_s^2) \quad (2)$$

where ω_r is the wave frequency, γ is the growth rate, k is the wave number in the horizontal direction, $V_d = E_{0z}/B$ is the horizontal drift speed, $\Psi_0 \equiv (\nu_e\nu_i)/(\Omega_e\Omega_i)$

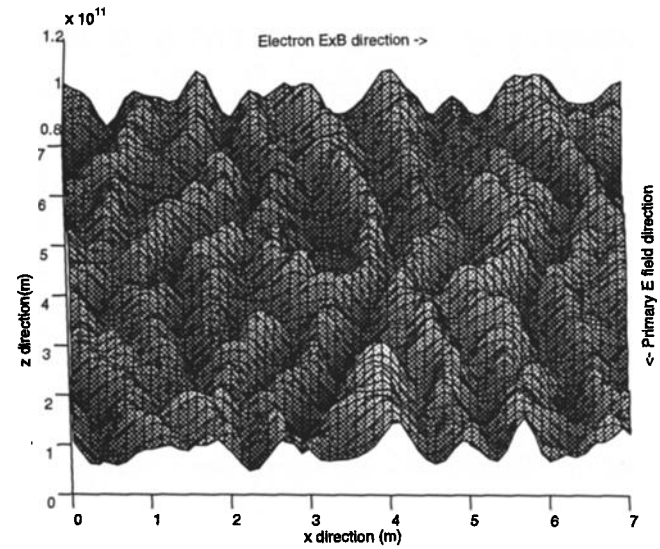

Figure 2. Density of waves in a saturated state.

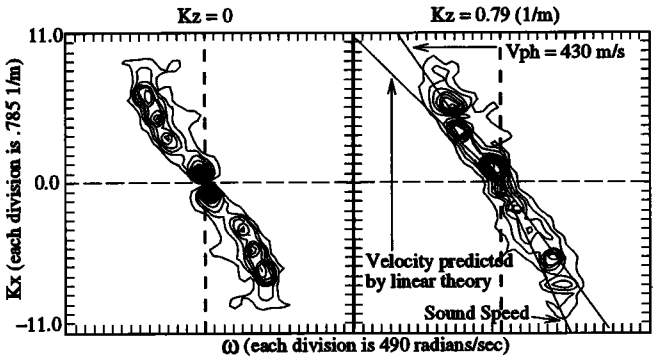

Figure 3. Two cross sections of the density power spectrum, $|\delta n(k_x, k_z, \omega)|^2$. A dispersion relationship between ω and (k_x, k_z) is evident. The left plot shows the $k_z = 0$ modes where the waves travel horizontally. The right plot shows modes with an $8m$ wavelength in the vertical direction. Note that the distance of the peak from $\omega = 0$ (ie. the Doppler shift) exceeds the spectral width, a typical characteristic of type I waves.

and $C_s \equiv \sqrt{(T_e + T_i)/m_i}$ is the acoustic speed. From this, the velocity predicted by linear theory is $610m/s$ and the acoustic speed is $C_s = 350m/s$. For all five simulations shown in Figure 1 the phase velocities range from C_s to $1.3C_s$. In two cases, when $T_e = 416K$ and in the lower resolution simulation where $E_{0y} = 15mV/m$, the waves travel at a speed slightly above C_s while for all the other simulations the dominant waves travel at a speed approaching $1.3C_s$. Interestingly, the value, 1.3, is close to a constant that arises frequently in the linear theory of the FB instability, $1 + \Psi_0 \approx 1.3$.

The simulations show an interesting relationship between the elevation angle and wave phase velocity as seen in Figure 4. This shows that the predominant mode does not travel in the direction of the drifting electrons as predicted by linear theory but, instead, travels at a small angle which increases as we increase the magnitude of the driving electric field.

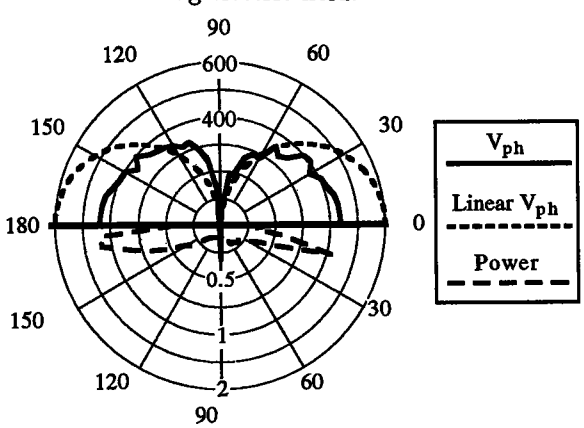

Figure 4. These plots show measurements from a simulated radar with a fixed $2m$ wavelength (scattering from $1m$ waves) as it sweeps from horizon to horizon. The theta axis refers to the angle above the horizon in degrees. The upper half of the figure graphs the phase velocity while the bottom half graphs the density power spectrum in arbitrary units. Both halves represent rightward traveling waves. The upper half of the plot tells us that the phase velocity remains relatively constant from horizontal to within 20 degrees of vertical. The upper dashed curve shows the phase velocities predicted by linear theory.

These simulations provide evidence that ion Landau damping may not play an important role in eliminating short wavelength modes. After saturation, the distribution of the ions in velocity space differs from the initial Gaussian profile by only an offset of its mean velocity due to the ion Pederson drift velocity. If ion Landau damping were important, one would expect to see a stretching of the distribution around the resonant frequency. The absence of this feature implies that a fluid model for ion behavior may be adequate.

Linearizing the electron behavior drastically changes the results of the simulations and thereby reveals the importance of the nonlinear $\kappa\hat{y}\cdot\nabla\phi\times\nabla n$ term in (1). In this case, the waves saturate at amplitudes almost an order of magnitude larger than those obtained in the baseline simulation. Figure 5 shows a typical density profile of the saturated waves obtained in a run with linearized electron behavior. Notice the monochromatic nature of the waves and, also, that the direction of wave propagation parallels the horizontal drift velocity direction. Finally, the velocity distribution of the ions shows the effects of ion heating and a stretching out of the distribution around the electron drift speed, a characteristic signature of Landau damping.

Particle noise effectively masks the instability for drift velocities substantially below the baseline case. Figure 1B shows the elevated saturation levels for two cases with drift velocities above the baseline case. Additionally, as the drift velocity increases, the principal mode develops a longer wavelength and a larger vertical component. The phase velocities of these modes increase only slightly with higher values of the drift velocity, far less than the amount predicted by linear theory.

The baseline case assumes isothermal electrons with $T_e = T_n$. This is not necessarily a good assumption and a more sophisticated model of electron kinetic effects may be necessary, particularly in the auroral electrojet. However, we find that changing the electron temperature drastically has a minimal effect on the behavior of the saturated waves. Figure 1A shows the time history of the density variations versus time for three electron temperatures. Even for these extreme cases, the effects are noticeable but not dramatic.

Viewing these simulations as movies reveals a number of additional features. First, small spatial scale

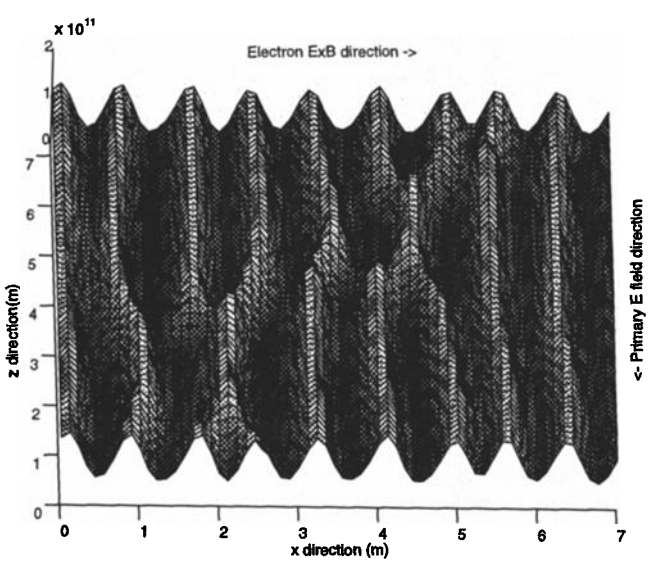

Figure 5. A snapshot of the density profile in the case where the electron behavior has been linearized.

waves can be seen traveling upward along the crests of the principal waves. Likewise small scale waves are observed traveling downward in the valleys. These are the nonlinear $\mathbf{E}\times\mathbf{B}$ effects with $\mathbf{E}$ arising from the field of the principal wave. Also, ripples and eddies form along the edges of the principal waves. These may be responsible for the turning of the waves off the direction of the drift velocity. Perturbation theory applied to either the maxima or the edges of the principal waves indicate that some of the secondary waves may also grow. This analysis will be addressed in a later paper. Movies generated from a number of these simulations may be accessed through the Internet via the MOSAIC program (URL: ftp://ee.cornell.edu/pub/jro/meers/fbi-movies.html)

Discussion and Conclusions

The results of our simulations agree well with the existing observations of type I waves. The phase velocities obtained from the numerical solutions are well below the velocity predicted by linear theory. This corroborates the observations of *Cohen and Bowles* [1967], *Hanuise and Crochet* [1981] and many others. The phase velocities remain almost constant within an extended range of elevation angles as first observed by *Cohen and Bowles* [1967]. We find the dominant waves to be quite monochromatic, a result confirmed by the rocket observation of *Pfaff et al.* [1987]. The nonlinearly induced vertical waves we see may explain the radar observations of *Kudeki et al.* [1987]. Additionally, the dominant waves do not travel strictly horizontally. The angle between the drift direction and the dominant wave of the system becomes larger as the driving electric field, E_{0y}, becomes more negative. These features are all caused, principally, by the nonlinear $\mathbf{E}\times\mathbf{B}$ term represented in the potential equation, (1), by the $\kappa\hat{\mathbf{y}}\cdot\nabla\phi\times\nabla n$. Dropping this term from the simulations has a profound effect on the solutions, an effect far greater than that caused by dramatically varying the electron temperature or the electron drift speed.

Previous numerical investigations of the FB instability by *Newman and Ott* [1981] and *Janhunen* [1994] saw the development of waves whose dominant mode travels at an angle with respect to the electron drift. Additionally, we see from these simulations that this angle increases with driving electric field. *Janhunen* [1994] claims to see FB waves traveling at the velocity predicted by linear theory, a result which disagrees with both the experimental database and a hybrid simulation we have done using his parameters. Since Janhunen modeled electron behavior with a computationally expensive PIC method, he had to use an unrealistic electron-ion mass ratio and could not run his simulations long enough to obtain waves in a saturated state. These facts may account for the discrepancy.

Our results raise a number of questions. Since the ion Landau damping effect of *Schmidt and Gary* [1973] does not seem to play an important role in eliminating short wavelength effects, what eliminates these modes so effectively? Why do the waves have such a strong vertical component and what is the relationship between this vertical component and the electron drift speed? What mechanism leads to saturation? Finally, what determines the phase velocity? We expect to answer some of these questions in forthcoming studies.

In summary, these simulations display a number of important nonlinear features including secondary waves traveling perpendicular to the principal FB waves, wave phase velocities close to the sound speed, and phase velocities almost independent of their elevation angle. The dominant mode does not travel exactly parallel to the electron drift direction and this angle increases with the driving electric field. These results appear to agree well with observations of FB waves. We plan to publish a more detailed comparison between the simulations and radar and rocket data in the near future.

Acknowledgments. The authors are grateful for the help and insights of C. Seyler, D. Farley, M. Kelley, D. Hysell, R. Mason, R. Sudan and I. Boyd. This work was supported by the IGPP program at Los Alamos (9-XA3-Q7557-1), NASA (NAGW-3010) and NSF (PYI atm9158072).

References

Buneman, O., Excitation of field aligned sound waves by electron streams, *Phys. Rev. Lett.*, *10*, 285, 1963.

Cohen, R., and K. L. Bowles, Secondary irregularities in the equatorial electrojet, *J. Geophys. Res.*, *72*, 885, 1967.

Farley, D. T., A plasma instability resulting in field-aligned irregularities in the ionosphere, *J. Geophys. Res.*, *68*, 6083, 1963.

Fejer, B. G., J. Providakes, and D. T. Farley, Theory of plasma waves in the auroral E region, *J. Geophys. Res.*, *89*, 7487, 1984.

Freund, R. W., and N. M. Nachtigal, An implementation of the qmr method based on coupled two-term recurrences, *SIAM Journal on Scientific Computing*, *15*, 1994.

Hanuise, C., and M. Crochet, 5-50m wavelength plasma instabilities in the equatorial electrojet 2. Two-stream conditions, *J. Geophys. Res.*, *86*, 3567, 1981.

Janhunen, P., Three-dimensional stabilization mechanism for the auroral Farley-Buneman instability, *J. Atmos. Terr. Phys.*, *54*, 1633, 1992.

Janhunen, P., Perpendicular particle simulation of the E region Farley-Buneman instability, *J. Geophys. Res.*, *99*, 11461, 1994.

Kelley, M. C., *The Earth's Ionosphere*, Academic Press, 1989.

Kudeki, E., B. G. Fejer, D. T. Farley, and C. Hanuise, The condor equatorial electrojet campaign, Radar results, *J. Geophys. Res.*, *92*, 13561, 1987.

Newman, A. L., and E. Ott, Nonlinear simulations of type I irregularities in the equatorial electrojet, *J. Geophys. Res.*, *86*, 6879, 1981.

Pfaff, R. F., M. C. Kelley, E. Kudeki, B. G. Fejer, and K. Baker, Electric field and plasma density measurements in the strongly driven daytime equatorial electrojet, 1. The unstable layer and gradient drift waves, *J. Geophys. Res.*, *92*, 13578, 1987.

Schmidt, M. J., and S. P. Gary, Density gradients and the Farley-Buneman instability, *J. Geophys. Res.*, *78*, 8261, 1973.

Sudan, R. N., J. Akinrimisi, and D. T. Farley, Generation of small-scale irregularities in the equatorial electrojet, *J. Geophys. Res.*, *78*, 1453, 1973.

Meers Oppenheim and Niels Otani, 304 ETC, Cornell University, Ithaca NY 14853 (email: meers@ee.cornell.edu)
Corrado Ronchi, Division of Environmental Studies, ENEA, C.R.E. Casaccia, Rome, ITALY

(received August 12, 1994; revised September 27, 1994; accepted November 16, 1994.)